Toxicology and Applied Pharmacology 280 (2014) 352–361

Contents lists available at ScienceDirect

Toxicology and Applied Pharmacology

journal homepage: www.elsevier.com/locate/ytaap

A revised model of ex-vivo reduction of hexavalent chromium in human and rodent gastric juices

Paul M. Schlosser *, Alan F. Sasso

U.S. Environmental Protection Agency, National Center for Environmental Assessment, Washington, DC, United States

ARTICLE INFO

Article history:
Received 24 March 2014
Revised 17 June 2014
Accepted 12 August 2014
Available online 20 August 2014

Keywords:
Hexavalent chromium
Reduction
Gastric juice
Mouse
Rat
Human

ABSTRACT

Chronic oral exposure to hexavalent chromium (Cr-VI) in drinking water has been shown to induce tumors in the mouse gastrointestinal (GI) tract and rat oral cavity. The same is not true for trivalent chromium (Cr-III). Thus reduction of Cr-VI to Cr-III in gastric juices is considered a protective mechanism, and it has been suggested that the difference between the rate of reduction among mice, rats, and humans could explain or predict differences in sensitivity to Cr-VI. We evaluated previously published models of gastric reduction and believe that they do not fully describe the data on reduction as a function of Cr-VI concentration, time, and (in humans) pH. The previous models are parsimonious in assuming only a single reducing agent in rodents and describing pH-dependence using a simple function. We present a revised model that assumes three pools of reducing agents in rats and mice with pH-dependence based on known speciation chemistry. While the revised model uses more fitted parameters than the original model, they are adequately identifiable given the available data, and the fit of the revised model to the full range of data is shown to be significantly improved. Hence the revised model should provide better predictions of Cr-VI reduction when integrated into a corresponding PBPK model.

Published by Elsevier Inc.

Introduction

Oral exposure to hexavalent chromium (Cr-VI) has been shown to induce tumors in the mouse gastrointestinal (GI) tract and rat oral cavity, while trivalent chromium (Cr-III) does not exhibit this carcinogenic potential (Stout et al., 2009). This difference in response is attributed in part to the much greater absorption (bioavailability) of Cr-VI vs. Cr-III (Febel et al., 2001; Kerger et al., 1996). As a result, the reduction reaction of Cr-VI to Cr-III in the gastrointestinal tract is considered to be a major pathway for detoxification in humans and rodents (De Flora et al., 2008). While small quantities of Cr-VI can be reduced rapidly in GI juices, larger amounts are reduced more slowly, or deplete the available reducing agents (Proctor et al., 2012). Reduction rates are also pH-dependent, becoming slower as pH increases (Kirman et al., 2013).

In this article we describe a revision of a mathematical model of Cr-VI reduction in gastric juices ex vivo. By itself such a model can lend some understanding of Cr-VI dosimetry, but to be quantitatively useful it must be integrated into PBPK models of kinetics in the GI and whole body, as depicted in Fig. 1. The kinetic equations and parameters from the ex vivo model are used to predict Cr-VI reduction rates in a GI tract (sub)model, which in this illustration is comprised of three compartments: stomach, duodenum, and jejunum. Ingestion of Cr-VI is described as an influx into the stomach compartment, where it can either be reduced or transferred to the next GI compartment. Compartment- and species-dependent GI characteristics which effect the rate of reduction include gastric emptying rates, lumen volumes, the mass of reducing agents (electron donors which reduce Cr-VI), and lumen pH. The GI-tract (or whole-body) model would also include the rate of reducing agent replenishment through ingestion and secretion into the lumen in gastric juices.

Reduction of Cr-VI, which occurs largely in the stomach, competes with the transfer of Cr-VI to the small intestine where it is absorbed. Reduction and gastric emptying occur simultaneously and the fraction of Cr-VI that is transferred and hence available for absorption depends on the relative rate of transfer vs. reduction. Thus the rate of absorption and hence cancer risk in humans as compared to rodents will be impacted by species differences in pH and the amount of reducing agents present. Accurate prediction of human cancer risks is likely to depend on accurately modeling the dependence of Cr-VI's reduction rate on these factors. Given the complexities and time-dependencies of Cr-VI in the whole body and the critical role of Cr-VI reduction in gastric juices, it makes sense to first model reduction in the isolated, ex vivo setting.

Proctor et al. (2012) developed a simple model of Cr-VI reduction kinetics for the rat and mouse at a single pH using kinetics measured ex vivo, which was then integrated into the PBPK model of Kirman et al. (2012). The PBPK model also incorporated a pH-dependence term based on experiments with human gastric juices ex vivo. Kirman et al. (2013) provide details of those human ex vivo kinetic data and describe their incorporation into a human PBPK model. These reduction models

* Corresponding author at: U.S. EPA, M.D. B243-01, RTP, NC 27711, United States. Fax: +1-919 685 3330.
E-mail address: schlosser.paul@epa.gov (P.M. Schlosser).

http://dx.doi.org/10.1016/j.taap.2014.08.010
0041-008X/Published by Elsevier Inc.

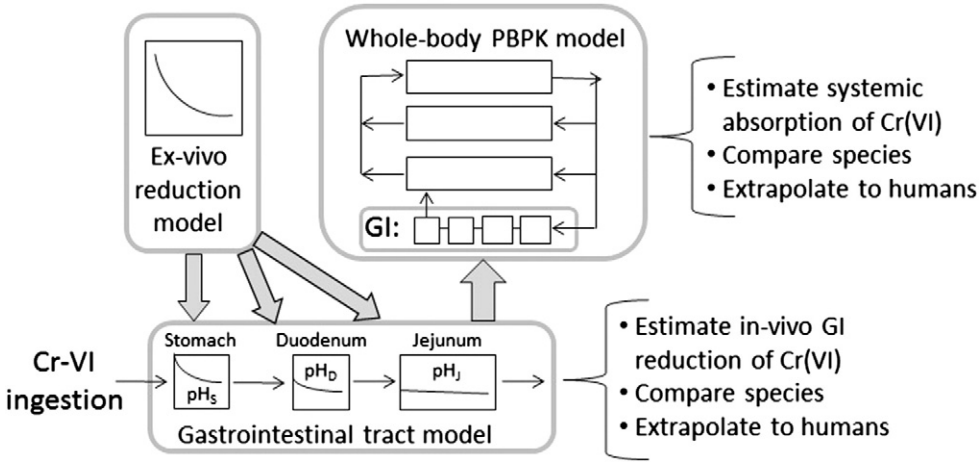

Fig. 1. Schematic of integration of ex vivo reduction kinetics into in vivo gastric and whole-body PBPK models.

assumed a single reducing agent and binary reaction constant. In the isolated ex vivo experiments the total amount of reducing agent is limited to the total amount present in the gastric juices and is eliminated stoichiometrically (one-to-one) with Cr-VI. The model does not consider the speciation of Cr-VI, which depends on both pH and total Cr-VI concentration (Brito et al., 1997). While Proctor et al. (2012) mention a number of reducing agents known to be present in gastric juices (ascorbate, glutathione, NADH, sulfhydryls), they used a simplified lumped-parameter model with a goal of parsimony. Close examination of their results, however, shows that the model adequately fits low concentration reduction data, but under-predicts the reduction observed at higher concentrations.

Like the previous model of Proctor et al. (2012) we assume that the stomach juices contain one or more reducing agents – electron donors – which react with Cr-VI chemical species to reduce Cr to Cr-III. It is clear from the data that one or more cofactors are available in limited supply, as small amounts of Cr-VI are very rapidly reduced, but the reduction rate diminishes with time, and this exhaustion of the cofactor(s) occurs more quickly at high initial Cr-VI concentrations. While ascorbate, glutathione, NADH, sulfhydryls can all serve as reducing agents, the specific concentrations of each of these in the stomach juices used to measure Cr-VI reduction (by Proctor et al., 2012, and Kirman et al., 2013) and their individual reaction rates with Cr-VI (species) are not known. Hence, like Proctor et al. (2012), we use here the generic term "reducing agents", and that aspect of the model is phenomenological.

We believe that there are several shortcomings in the previous models which can be improved upon. The pH-dependence was evaluated by Kirman et al. (2013) by separately fitting the reduction data at each pH (and each Cr-VI concentration and dilution of gastric juices) using the same reduction model, thereby obtaining a different value of the effective binary rate constant, k_{eff}, for each experimental condition. When the authors plotted the binary constants obtained this way vs. pH, k_{eff} was observed to roughly vary as exp(−pH); i.e., k_{eff} was assumed to equal $k_{0g} \cdot \exp(-\mathrm{pH})$, where k_{0g} is a pH-independent rate constant. However this is only an empirical observation, since pH is defined as the base-10 logarithm of $1/[H^+]$ and a direct relationship between reduction rate and proton concentration is not expected. Further, the k_{eff} obtained by fitting the reduction data at pH = 1 is 3-fold lower than that obtained using the pH = 1.3 data, a difference not consistent with the assumed pH-dependence, which predicts a 35% higher value at pH = 1 vs. 1.3. At pH = 4, two values of k_{eff} were obtained that differed by a factor of 5, from fitting k_{eff} to two data sets obtained at different dilutions of gastric juice and initial Cr-VI concentration, indicating a dependence on other experimental variables (dilution of gastric juices or Cr-VI concentration) that the model does not capture.

In our revised model, we attempt to describe the pH-dependence based on the observed pH-dependent speciation of Cr-VI, assuming that differences in the reduction rate occur due to the shift in relative abundance of specific forms of Cr-VI. According to Brito et al. (1997), chromate(VI) in aqueous solution appears primarily as one of three forms at pH > 3: chromate (CrO_4^{2-}), hydrogen chromate ($HCrO_4^-$), and dichromate ($Cr_2O_7^{2-}$). At pH < 3, hydrogen dichromate ($HCr_2O_7^-$) and chromic acid (H_2CrO_4) also become significant. In particular, the concentration fractions of $HCrO_4^-$ and $Cr_2O_7^{2-}$ decline significantly for pH > 5, converting to CrO_4^{2-}. So, in particular, we assumed that either $HCrO_4^-$ or $Cr_2O_7^{2-}$ was the predominant substrate for reduction since they are predominant at low pH; i.e., that the reduction rate of Cr-VI decreases with increasing pH because $HCrO_4^-$ or $Cr_2O_7^{2-}$ is the form which participates in the reduction reaction, and as pH increases the amount of Cr-VI present in these forms decreases. By using this mechanism-based model of pH-dependence, it may be possible to more accurately describe the observed variation in reduction rates with pH.

Since the concentration-dependence of Cr-VI reduction appeared to be not completely captured by Proctor et al. (2012), additional pools of reducing agents were also considered, with the number of pools evaluated separately for mice, rats, and humans, based on the model's ability to fit the data for that species.

Material and methods

The experimental design and methodology are described in Proctor et al. (2012) and Kirman et al. (2013). The source data were graciously made available by the study authors. Modeling and analysis for this current work were performed using acslX software (version 3.0.2.1, Aegis Technologies, Huntsville, AL). The .csl file is included as supplementary material.

Original model. As stated in the Introduction, the reduction model used by Proctor et al. (2012) and Kirman et al. (2013) assumed a single reducing agent (electron donor) pool, with the agent participating in a binary reaction with Cr-VI:

$$\text{reduction rate} = k_{\text{eff}}[\text{R}] \cdot [\text{Cr-VI}],$$

$$\text{hence}: \quad \frac{\mathrm{d}[\text{Cr}-\text{VI}]}{\mathrm{d}t} = \frac{\mathrm{d}[\text{R}]}{\mathrm{d}t} = -k_{\text{eff}}[\text{R}] \cdot [\text{Cr-VI}],$$

where [Cr-VI] is the total concentration of Cr-VI present, in all chemical forms and [R] is the concentration of the reducing agent. R was assumed to have an initial concentration, $[\text{R}]_{\text{initial}}$, which was adjusted to fit the experimental data along with the binary rate constant, k_{eff}. Proctor et al.

(2012) developed and described their modeling in exactly this form, using "K" for k_{eff}, and obtained $k_{eff} = 0.004983\ L \cdot mg^{-1} \cdot min^{-1}$ (reported as $0.3\ L \cdot mg^{-1} \cdot h^{-1}$) and $[R]_{initial} = 15.74\ mg \cdot L^{-1}$ for the rat and $k_{eff} = 0.003295\ L \cdot mg^{-1} \cdot min^{-1}$ (reported as $0.2\ L \cdot mg^{-1} \cdot h^{-1}$) and $[R]_{initial} = 16.64\ mg \cdot L^{-1}$ for the mouse (exact values from personal communication). Since the experiments of Proctor et al. (2012) were conducted with rodent gastric juices diluted 10-fold, and we chose to build the dilution adjustment explicitly into our assumptions, these values of $[R]_{initial}$ were converted to un-diluted values, $R_0 = 157.4$ and $166.4\ mg \cdot L^{-1}$ for the rat and mouse, respectively.

Kirman et al. (2013) conducted experiments at multiple dilutions and pH values and used the symbol "K_{red}". To estimate the reduction rate constant for each pH/dilution combination, the corresponding reduction time-course was fitted with

$$k_{eff}(\text{or } K_{red}) = k_{gastrict} \cdot \text{dil}$$

where $k_{gastric}$ was assumed to be the effective constant for undiluted gastric juices and dil is the fold dilution. The initial concentration of reducing agent was set as $[R]_{initial} = R_0/\text{dil}$, where R_0 is the initial concentration in undiluted gastric juices. After obtaining values of $k_{gastric}$ for each dilution and pH value, these values were plotted vs. pH and a function was fit to the resulting values, as:

$$k_{gastrict} = k_{0g} \cdot \exp(-\text{pH}).$$

Hence the reduction model of Kirman et al. (2013) as used in fitting the ex vivo reduction data can be summarized as:

$$k_{eff} = k_{0g} \cdot \exp(-\text{pH}) \cdot \text{dil and } R_0/\text{dil},$$

given the reduction rate and differential equations listed above. Kirman et al. (2013) obtained $k_{0g} = 44.5\ L \cdot mg^{-1} \cdot h^{-1} = 0.742\ L \cdot mg^{-1} \cdot min^{-1}$ for humans. Separate values of R_0 were fit to each data set they examined; the mean of these is $7.27\ mg \cdot L^{-1}$ (exact value based on results provided by Dr. Kirman and colleagues).

Comparison of original and revised models. Our alternate model, described below, is compared to the results of Kirman et al. (2013) by showing model fits to individual experiments. For our model, we performed a global optimization over all data sets simultaneously, with the dependence on pH and dilution built into the model. Therefore, our data-set-specific rate constants are not distinct from the overall regression but are defined by it. Since the model form used by Kirman et al. (2013) for the in vivo PBPK model is defined by $k_{eff} = k_{0g} \cdot \exp(-\text{pH}) \cdot \text{dil}$ (with dil = 1, corresponding to the regression line shown in Fig. 2C of their publication), an appropriate test and comparison of their model is therefore to use the k_{eff} defined by that regression line. This was preferred to using the data-set-specific rate constants indicated as points in the published figure panel.

pH-dependence. As discussed in the Introduction, we sought to describe the pH-dependence of Cr-VI reduction mechanistically, based on the corresponding pH-dependent chemical equilibria among Cr-VI forms. Chromate speciation equilibria can be described by four reversible reactions (Brito et al., 1997):

$$CrO_4^{2-} + H^+ \underset{\leftarrow}{\rightarrow} HCrO_4^-;\ K_{11} = \frac{[HCrO_4^-]}{[CrO_4^{2-}][H^+]} \quad (1)$$

$$2HCrO_4^- \underset{\leftarrow}{\rightarrow} Cr_2O_7^{2-} + H_2O;\ K_{22} = \frac{[Cr_2O_7^{2-}]}{[HCrO_4^-]^2} \quad (2)$$

$$HCrO_4^- + H^+ \underset{\leftarrow}{\rightarrow} H_2CrO_4;\ K_{21} = \frac{[H_2CrO_4]}{[HCrO_4^-][H^+]} \quad (3)$$

$$Cr_2O_7^{2-} + H^+ \underset{\leftarrow}{\rightarrow} HCr_2O_7^-;\ K_{32} = \frac{[HCr_2O_7^-]}{[Cr_2O_7^{2-}][H^+]} \quad (4)$$

While we would prefer to use separate forward and reverse reaction rates for each of these, separate rate constants were not available. Therefore we chose to assume that these reactions are relatively fast compared to reduction, hence can be treated as at equilibrium.

Since only the total amount of Cr-VI is known (either as the initial amount added or calculated as what remains after a given degree of reduction), the set of equilibrium equations, (1)–(4), must be solved simultaneously to determine the concentration of each chromium species: $[CrO_4^{2-}]$, $[HCrO_4^-]$, $[Cr_2O_7^{2-}]$, $[H_2CrO_4]$, and $[HCr_2O_7^-]$. Given the pH (i.e., $[H^+]$) and mass balance for total Cr-VI,

$[CrO_4^{2-}] + [HCrO_4^-] + [H_2CrO_4] + 2[Cr_2O_7^{2-}] + 2[HCr_2O_7^-] = [\text{Cr-VI}]_{Total}$,

these can be solved algebraically for the individual chemical species concentrations as a function of $[\text{Cr-VI}]_{Total}$, for example:

$$\left[CrO_4^{2-}\right] = \frac{-B + \sqrt{B^2 + 4 \cdot A \cdot [\text{Cr-VI}]_{Total}}}{2 \cdot A}$$

where

$$A = 2 \cdot K_{22} \cdot \left(K_{11} \cdot \left[H^+\right]\right)^2 \cdot \left(1 + K_{32} \cdot \left[H^+\right]\right),$$

$$B = 1 + K_{11} \cdot \left[H^+\right] \cdot \left(1 + K_{21} \cdot \left[H^+\right]\right),$$

$$[HCrO_4^-] = K_{11} \cdot \left[H^+\right] \cdot \left[CrO_2^{4-}\right],$$

$$[H_2CrO_4] = K_{21} \cdot \left[H^+\right] \cdot [HCrO_4^-],$$

$$\left[Cr_2O_7^{2-}\right] = K_{22} \cdot [HCrO_4^-]^2,$$

and

$$[HCr_2O_7] = K_{32} \cdot \left[H^+\right] \cdot \left[Cr_2O_7^{2-}\right] = K_{32} \cdot K_{22} \cdot \left[H^+\right] \cdot [HCrO_4^-]^2.$$

Brito et al. (1997) obtained values of $K_{11} = 7.73 \times 10^5\ M^{-1}$ ($pK_{11} = \log_{10}(K_{11}) = 5.888$), $K_{22} = 132\ M^{-1}$ ($pK_{22} = 2.12$), $K_{21} = 13.2$ ($pK_{21} = 1.12$), and $K_{32} = 15.2$ ($pK_{32} = 1.28$). For the concentration range examined by Kirman et al. (2013) with human gastric juices, $[\text{Cr-VI}]_{Total} = 0.1\text{–}2\ mg/L \sim 2 \times 10^{-5}\text{–}4 \times 10^{-6}\ M$, and with these equilibrium constants, no more than 1% of the total chromate is calculated to appear as dichromate. At the higher concentrations used by Proctor et al. (2012) with mouse and rat gastric juices, a large fraction appears as dichromate; i.e., 14% of total Cr-VI is in this form for 40 mg/L total Cr-VI at pH = 4.

We considered the possibility that dichromate is the primary reactive species. However, given the chemistry described above, $[Cr_2O_7^{2-}]$ varies roughly as the square of $[\text{Cr-VI}]_{Total}$ in the concentration range studied. If the kinetics were modeled as being proportional to $[Cr_2O_7^{2-}]$, the resulting $[\text{Cr-VI}]_{Total}$ vs. time curves differed significantly in shape from those obtained when hydrogen chromate was assumed to be the reactant. Model predictions based on this assumption were clearly not consistent with the data of Proctor et al. (2012) and Kirman et al. (2013) (results not shown). When we attempted to fit a model that allowed both chemical species to react, the rate constant for the dichromate-dependent term converged to zero. These results were considered strong evidence that dichromate was not the direct reactant.

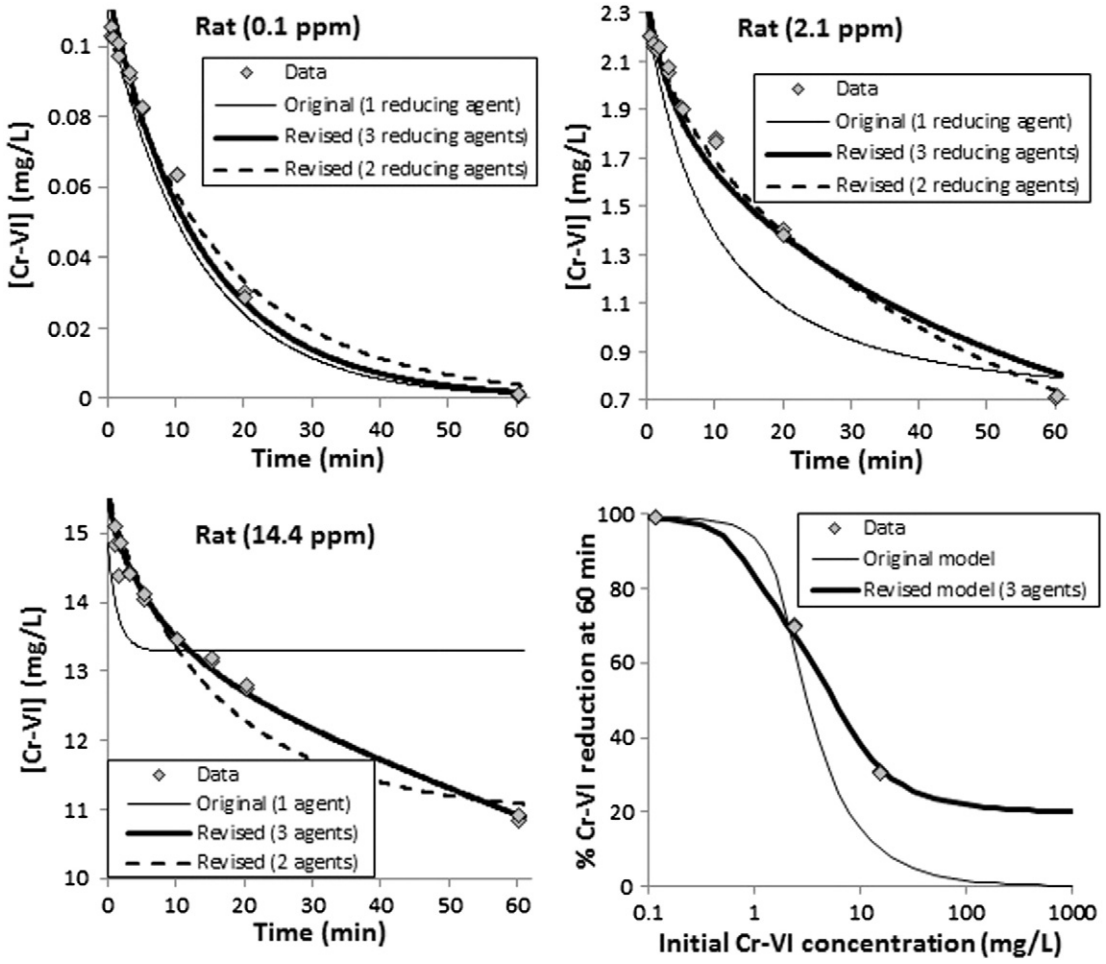

Fig. 2. Ex-vivo model predictions in the rat for different reaction schemes. Data in first three panels were used for calibration; data in the lower-right panel were not used for calibration. Two of the revised rat parameters were fixed to values from the mouse model. An improved model fit at high initial Cr-VI concentrations is achieved by assuming additional reducing agents are present in the gastric fluid and contents. At low concentration, minimal improvement is achieved (the 2- and 3-reducing agent model results are indistinguishable at 0.1 ppm). Data graciously provided by Summit Toxicology and ToxStrategies, Inc.

Using the equilibrium constants reported by Brito et al. (1997), the equations above predict that at 1 mg/L total Cr-VI, $HCrO_4^-$ represents 43% of total Cr-VI at pH = 1, 98.3% at pH = 4, and 7.2% at pH = 7. Thus, $HCrO_4^-$ is a species whose relative abundance decreases at higher pH values (above pH = 4) and this shift in its relative abundance might explain the pH-dependence of the reduction rate. However, while the shift in abundance for $HCrO_4^-$ is qualitatively closer to the empirical data of Kirman et al. (2013), the difference in $HCrO_4^-$ abundance between pH = 4 and 7, 13.7-fold, is much less than the change in Cr-VI reduction rate observed by Kirman, et al. (2013) (30–160 fold). Further, between pH = 4 and 1, the equilibrium chemistry predicts a decrease of 56% in $[HCrO_4^-]$, but the empirical constants of Kirman et al. (2013) increased by 2–3 fold.

Therefore we relaxed our initial assumption to include the possibility that H_2CrO_4 was equally or more reactive than $HCrO_4^-$, but this still did not provide a good fit to all of the data. The qualitative change in reaction rate with pH matches the observed data with this relaxed assumption, but the quantitative differences in reaction rate were not adequately captured. Given that the assumption of a binary reaction with one more reducing agents was probably also a simplification, we therefore decided to test this model with one of the equilibrium constants being adjusted in order to fit the full data set. Since we had determined the data to be not consistent with dichromate as a reactant species (see above), the pH-dependence seemed likely to be most influenced by the balance between $HCrO_4^-$ and CrO_4^{2-}, which depends most directly on K_{11}. Hence we assumed that varying K_{11} would provide a good fit to the full data set without varying any of the other parameters. However, when only K_{11} was varied and H_2CrO_4 and $HCrO_4^-$ were assumed to be equally reactive we found that we could adequately fit the data from pH = 1 to pH = 4, but that the reaction rate at pH = 7 was now under-predicted. Since $[CrO_4^{2-}]$ becomes significant at pH > 5, our final assumption was to allow CrO_4^{2-} to have a reactivity defined as a fraction, *f*, of that for H_2CrO_4 and $HCrO_4^-$.

In summary, for each reducing agent pool, R_{pool}, the rate of reduction was defined as:

$$\text{reduction rate} = k_{pool} \cdot \left[R_{pool}\right] \cdot \left(\left[H_2CrO_4\right] + \left[HCrO_4^-\right] + f \cdot \left[CrO_4^{2-}\right]\right).$$

Like Kirman et al. (2013), we found that the human reduction data were adequately described assuming a single pool of reducing agent, whose concentration in *undiluted* gastric juice is represented as $R_{0,1}$, with the initial concentration in a given experiment set as $R_{0,1}$/dil. While we believe it likely that human gastric juices contain multiple pools of reducing agents, just as appears to be the case in rodents (see below), the range of concentrations evaluated in the human data set is not sufficient to allow unique identification of parameters for multiple pools. If we attempt to fit a model with two or three pools to the human data, the parameter estimation does not properly converge because the fast reducing agent pool is never depleted and its rate masks those for any slower pools. To state this another way, if reduction by human gastric juices occurs via three

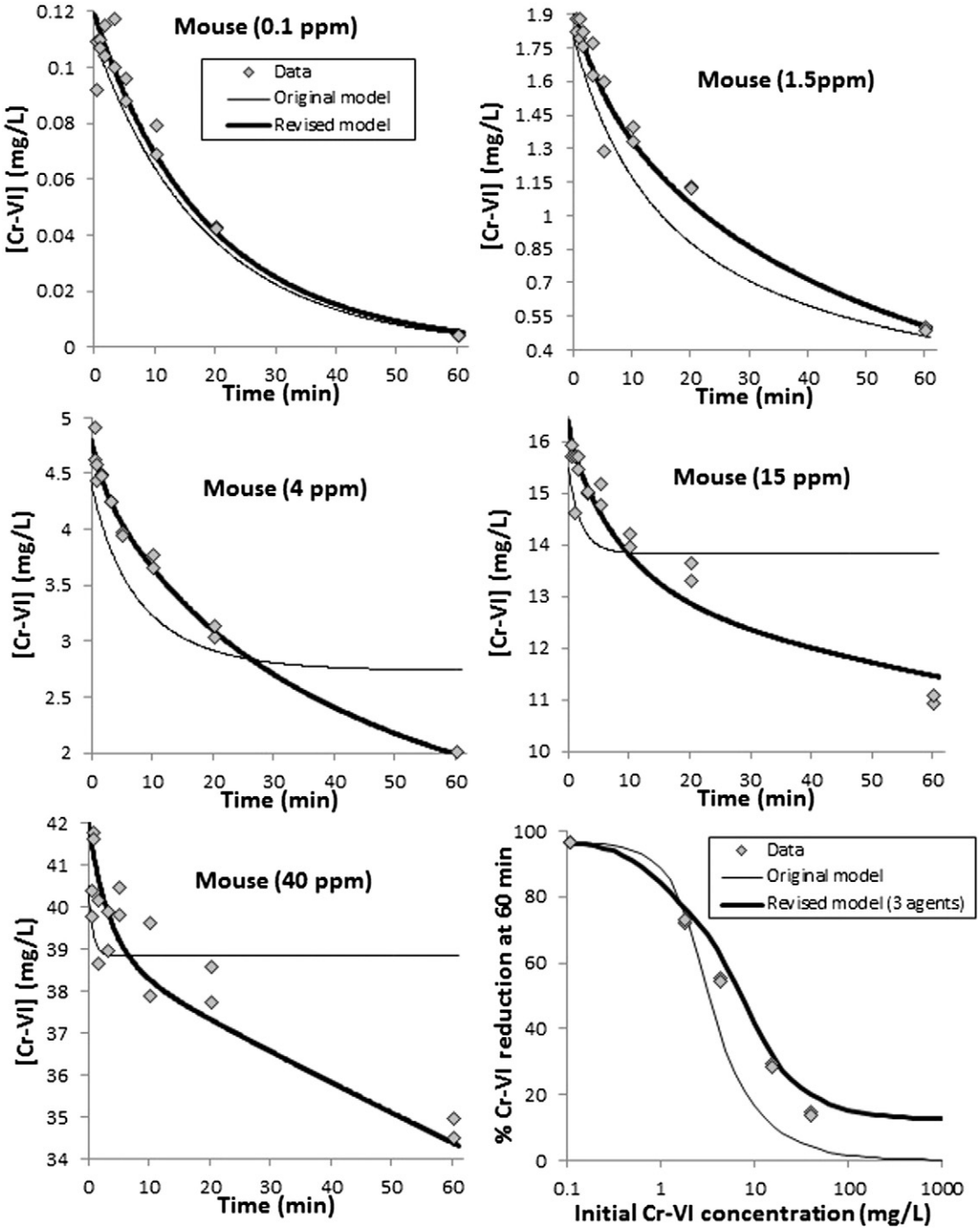

Fig. 3. Ex-vivo model predictions in the mouse for different reaction schemes. The original and revised 3-reducing agent models are presented. Data in first five panels were used for calibration; data in the lower-right panel were not used for calibration. As with the rat, the single reducing agent model deviates most from the data at high initial Cr-VI concentrations. Data graciously provided by Summit Toxicology and ToxStrategies, Inc.

reducing agents, but the rate for each is effectively first order because none of them becomes depleted (i.e., with rate constants k_{p1}, k_{p2}, and k_{p3}), then the rate of reduction is indistinguishable from what would occur with a single pool whose rate constant is the sum of the constants for the three pools; i.e., $k_1 = k_{p1} + k_{p2} + k_{p3}$. Since the parameters are fitted to the empirical reduction data, the human rate constant, k_1, and (undiluted) pool size, $R_{0,1}$, effectively incorporate reduction by all human reducing agent pools. Since the human exposures which will ultimately be evaluated for risk analysis are much lower than those used in the rodent bioassays, we believe this simplification of the human model, to only have one *effective* reducing agent pool, will be adequate.

Hence $k_{pool} = k_1$ and $R_{pool} = R_1$ for the single effective reducing agent pool for humans, with the initial concentration of reducing agent in undiluted gastric juice being $R_{0,1}$. Our human reduction model is then:

$$\text{reduction rate} = k_1 \cdot [R_1] \cdot \left([H_2CrO_4] + [HCrO_4^-] + f \cdot \left[CrO_4^{2-} \right] \right),$$

$$[R_1]_{initial} = R_{0.1}/\text{dil},$$

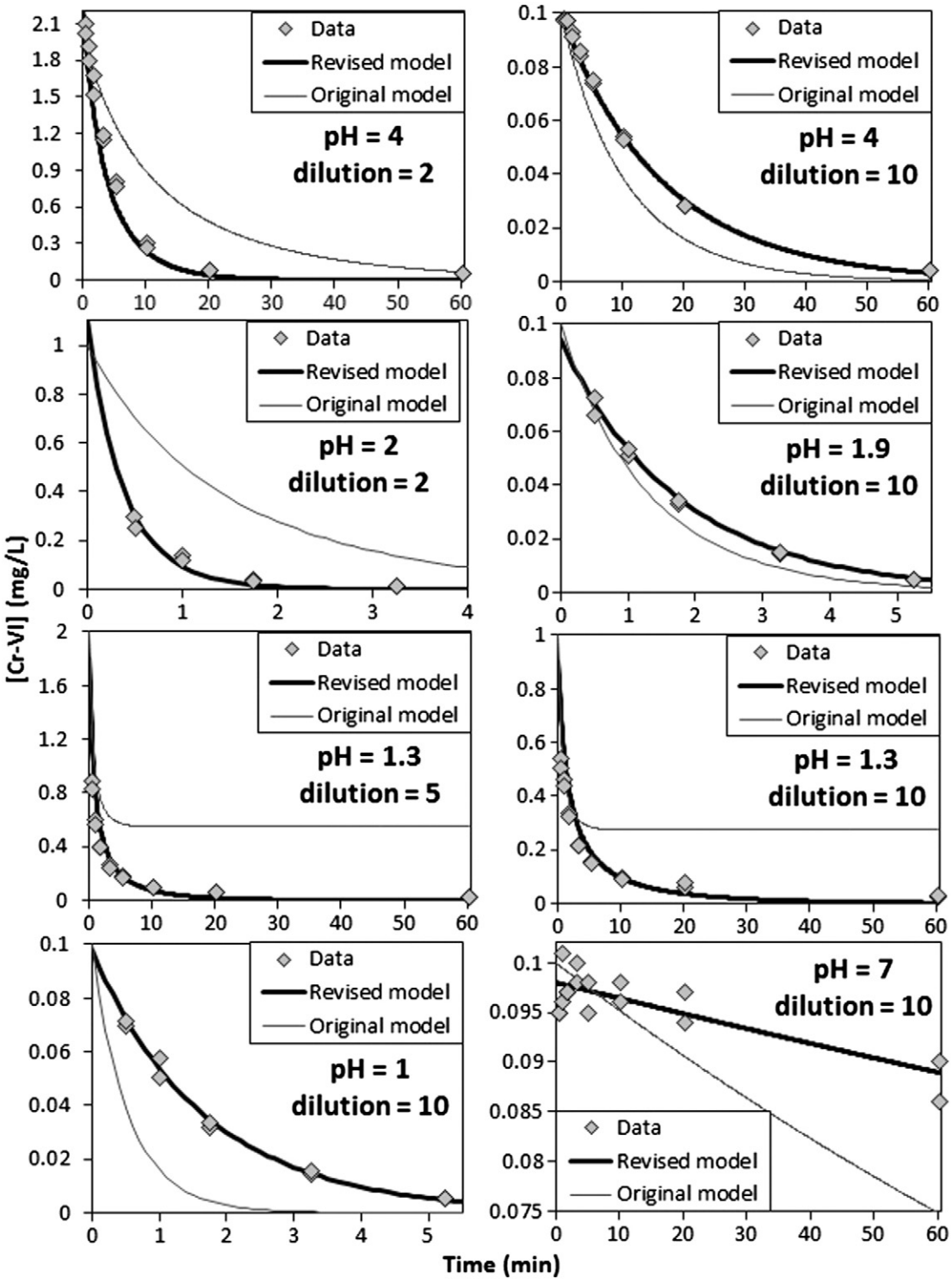

Fig. 4. Ex-vivo model predictions in the human. The original and revised models are presented. Note changes in initial concentration and time scale between panels. Both models assume a single reducing agent. At high initial Cr-VI concentration, the original model under-predicts reduction when compared to the revised model. This is most apparent at low pH, where the reduction rate is the fastest. At low initial Cr-VI concentrations, the single reducing agent model tends to over-predict the rate of reduction. Data graciously provided by Summit Toxicology and ToxStrategies, Inc.

with the chromium species concentrations being determined from the total Cr-VI concentration as a function of pH, as described above. In comparison, the model of Kirman et al. (2013) is:

$$\text{reduction rate} = k_{0g} \cdot \text{dil} \cdot [R_1] \cdot [Cr{-}VI]_{Total} \cdot \exp(-\text{pH})$$
$$[R_1]_{initial} = R_{0.1}/\text{dil}.$$

In summary, the two key differences between our model and that of Kirman et al. (2013) are: 1) we assume the leading rate constant, k_1, does not change with dilution while Kirman et al. (2013) assumed that their effective rate constant, $k_{0g} \cdot \text{dil}$, increases in direct proportion with gastric juice dilution; and 2) the pH dependence. The usual assumption for chemical kinetics is that rate constants are not altered by dilution of the reactants and the dependence on pH we have

incorporated is based on the pH-dependent chemistry of the chromate species. The fitted global parameters for the human data were then K_{11}, k_1, $R_{0,1}$, and f.

Initial concentrations. We also noted, however, that some of the time-course data were not consistent with the nominal targeted initial Cr-VI concentration. For example, the first two data points (from repeat experiments) for the set at pH = 4, dil = 2, and a target concentration of 2 mg/L had measured concentrations of 2.10 and 2.02 mg/L at 0.5 min; i.e., greater than what should have been the initial concentration. With the initial reduction rate for this experiment being very rapid, $[\text{Cr-VI}]_{\text{Total}}$ dropping to ~1.6 mg/L by 1.75 min, these data appear consistent with an initial concentration somewhat higher than 2 mg/L. Forcing the model to fit these data with an assumed initial concentration of 2 mg/L was found to create a bias in the predicted reaction rate, tending to a rate slower than exhibited by the data *after* those initial measurements. While less dramatic, the data for pH = 4, dil = 10, with an initial target concentration of 0.1 mg/L $[\text{Cr-VI}]_{\text{Total}}$, also appeared more consistent with an initial concentration slightly higher than the target. Other data sets appeared consistent with initial concentrations lower than targeted.

We assumed that these apparent discrepancies were most likely due to the difficulty of quickly mixing the reagents and then sampling the reaction at such short times, and therefore thought it appropriate to allow the modeled initial concentration for each experiment to vary up to 10% from the targeted concentration. This allowed the model to better capture the observed initial reaction rates (slope of concentration vs. time data), which is the critical information contained in the data.

Since the human data included 9 experiments (combinations of pH, dilution level, and initial chromate concentration), a total of 13 parameters were allowed to vary in fitting those data: the 4 global parameters (K_{11}, k_1, $R_{0,1}$, and f) and the initial concentration for each of the 9 experiments (constrained to be within 10% of the target concentration). The 9 data sets contained a total of 122 measurements, ranging from 10 to 17 per experiment, so there were just over 9 data points per fitted parameter.

Reducing agent pools. As stated in the introduction, the reduction model used by Proctor et al. (2012) and Kirman et al. (2013) assumed a single reducing agent (electron donor) pool, with the agent participating in a binary reaction with Cr-VI. The reducing agent was assumed to have an initial concentration, R_0, which was adjusted to fit the experimental data along with the binary rate constant, k_{eff}. While the assumption of a single reducing agent allowed for adequate model fits to the lower concentration data from the ex vivo rodent experiments, closer examination of the fits to the high concentration (specifically, plotting the results with a linear y axis), showed that the amount of reduction observed with higher initial Cr-VI concentrations was significantly under-predicted (Figs. 2–5). More specifically, while those data showed an initial rapid reduction that was somewhat consistent with the single pool model, after the first 5–10 min, when the single-pool model predicts that reduction would cease due to depletion of the reducing agent, the data show continued reduction, although at a slower rate. Therefore we added terms to the model corresponding to additional pools of reducing agent, but only so far as these resulted in significant improvement in model fits.

While the rodent reduction experiments were all conducted at a single pH, we used the chromate speciation chemistry and relative contributions determined from fitting the human reduction data. Inclusion of this pH-dependence is ultimately necessary for application of the model to reduction *in vivo*, since pH changes between sections of the rodent GI tract (DeSesso and Jacobson, 2001; Kararli, 1995). In addition to the initial one-pool model, three other options were evaluated: a) two reducing agents (two-pool model) with corresponding defined initial pool sizes (concentration of reducing agent pre-reaction); b) three reducing agents (three-pool model) with corresponding defined pool sizes;

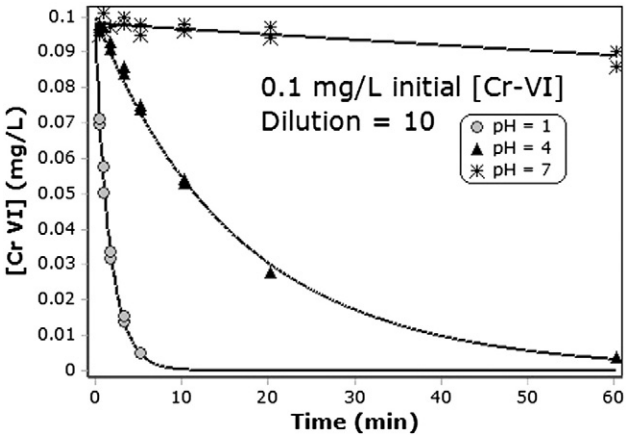

Fig. 5. Performance of the revised ex-vivo kinetic model in humans across a wide pH range. Data graciously provided by Summit Toxicology and ToxStrategies, Inc.

c) three-pool model, but where the size of the third pool is sufficiently large that it is not significantly depleted for the experimental conditions evaluated. For this third case an effective first-order rate constant, k_{vsf}, replaces the product of a binary rate constant, k_{vs}, and the concentration of the pool, $[R_{\text{vs}}]$; i.e., k_{vsf}, $= k_{\text{vs}} \cdot [R_{\text{vs}}]$. This third option reduces the number of fitted parameters by one vs. the full three-pool model, since the initial size of the third pool does not need to be estimated. The reduction rate equations for the three options are:

a) two reducing agents: $r_{\text{red}} = (k_f[R_f] + k_s \cdot [R_s]) \cdot ([H_2CrO_4] + [HCrO_4] + f \cdot [CrO_4^{2-}])$;

b) three reducing agents with finite third pool: $r_{\text{red}} = (k_f[R_f] + k_s \cdot [R_s] + k_{vs} \cdot [R_{vs}]) \cdot ([H_2CrO_4] + [HCrO_4^{2-}])$;

c) three reducing agents with unknown or effectively unlimited third pool: $r_{\text{red}} = (k_f[R_f] + k_s \cdot [R_s] + k_{vsf}) \cdot ([H_2CrO_4] + [HCrO_4] + f \cdot [CrO_4^{2-}])$.

Here the subscript "f" indicates a pool that is expected to react and be depleted quickly (fast), "s" indicates a pool that reacts and is depleted (more) slowly, and "vs" one that reacts and is depleted very slowly. Note that we are *not* suggesting that there is actually an infinite reducing capacity in the 3rd pool for option (c), just that the concentrations of Cr-VI used in the experiments are not sufficiently high to significantly deplete this third pool, hence the size of the pool cannot be estimated using the data and it can be treated as unlimited in the concentration range being analyzed.

Before describing our results, the number of data points used per fitted parameter should be evaluated to determine if the parameter estimation is sufficiently supported. The parameters that determine the speciation of chromate, and the fractional contribution of CrO_4^{2-} (i.e., f) were determined using the human data as described above and assumed to be identical for rodents, hence not further adjusted. Thus in fitting the options above (for mice or rats), (a) involved four kinetic parameters (k_f, $R_{0,f}$, k_s, and $R_{0,s}$), (b) involved 6 kinetic parameters (those for (a) plus k_{vs} and $R_{0,vs}$), and (c) involved 5 kinetic parameters (those for (a) plus k_{vsf}). For the mouse, data were available for 5 initial chromate concentrations, which were also fitted. Hence option (a), (b), and (c) involved adjustment of 9, 11, and 10 parameters, respectively. The 5 mouse data sets included a total of 84 measurements (16–18 per set); hence the number of data points per parameter was 9.3, 7.6, and 8.4 for (a), (b), and (c), respectively.

For the rat there were only 3 chromate concentration data sets, so in evaluating among the options a total of 7, 9, and 8 parameters were adjusted for (a), (b), and (c), respectively, with a total of 49 data points. Hence option (b) only had 5.4 data points per parameter. However,

we also evaluated the fit of option (c) with k_f and k_s fixed at the values estimated from modeling the mouse data, reducing the number fitted for the rat option (c) to 6 parameters, thus with just over 8 data points per parameter. In combination, applying option (c) to both the mouse and rat data sets used 133 data points and 16 parameters (8 being constrained), or 8.3 points per parameter.

Results

Parameter optimizations were independently performed for rodents applying each of the three options above using the Nelder–Mead algorithm in acslXtreme. Both option (b) and option (c) provided significant improvement over option (a). However, option (b) did not produce sufficiently superior results over option (c), and parameters for the third reaction (k_{vs} and $R_{0,vs}$) were not uniquely identifiable. Only the single product term could be optimized (essentially k_{vsf}). Therefore, option (c) was determined to be the best model structure for rodents. As indicated above, we interpret option (c) as indicating that the size of the third pool is simply much larger than the concentration range used in these experiments, so its concentration cannot be estimated with reasonable accuracy using model form (b).

For the rat it was found that there was not a significant improvement in fit when k_f and k_s were varied vs. fixed at the values estimated for the mouse (results with these two fitted separately for the rat not shown). Hence their values listed in Table 1 are identical for mice and rats.

Fig. 2 illustrates the differences in model predictions between the original assumption (one reducing agent), and the revised two- and three-reducing agent schemes for the rat. Fig. 3 illustrates the original and revised (three-reducing agent) model results for the mouse. For the human, a single reducing agent pool assumption was adequate, since the addition of two or three pools did not sufficiently improve the model, and the additional parameters were non-identifiable. However, the revised, more mechanistic model structure and re-optimization of parameters resulted in significantly improved model fits over the original model. Results for the human are presented in Figs. 4–5. The final ex-vivo kinetic parameters for all species are contained in Table 1.

Examining the kinetic *data* for rats and mice shown in Figs. 2 and 3, one can see that at the highest initial Cr-VI concentrations there is significant reduction between 20 and 60 min, with no clear evidence that the reducing capacity has been depleted or saturated. The data and the revised model are consistent with continued reduction beyond 60 min and clearly inconsistent with the predictions of the original, one-pool model. This inconsistency was not evident in the publication of Proctor et al. (2012) because of the compressed, log-y axis used in their plots. Depletion of 100% reducing capacity in rodents at high concentration is only estimated by the original single reducing agent model, and could be shown at later time points or with yet higher Cr-VI concentrations. But based on these on these results it appears that use of the original reduction model may result in over-estimation of internal doses of Cr-VI when incorporated into a rodent physiologically-based pharmacokinetic model, because it under-estimates reduction in the 20–60 min time-frame.

Similar to the rodent, the original reaction scheme predicts reducing agent depletion at high concentration in the human (Fig. 4). Despite being limited to only a single reducing agent pool, the revised model more closely reproduces the data, and does not predict a complete depletion of reducing agent in the Cr-VI concentration range used. It should be noted, though, that the highest Cr-VI concentration used in the human ex-vivo experiments was 2 mg/L in a gastric juice sample diluted only 2-fold, while the rat experiments were conducted up to 16 mg/L and the mouse up to 42 mg/L, in gastric juice samples diluted 10-fold. Hence the rodent data were sufficient to show multiphase depletion curves consistent with multiple pools of reducing agent, while the human data were not. The revised ex-vivo model also gives a mechanistic understanding of the pH-dependence of Cr-VI reduction. Although several parameters had to be adjusted to fit the human ex-vivo data, it captures the pH-dependence in the experimental data much more accurately. If incorporated into a PBPK model (work ongoing), the revised reaction scheme should provide an improved analysis of the effect of stomach pH variations on Cr-VI reduction.

It has been previously suggested that at high Cr-VI concentrations in rodent gastric juice, the reducing capacity is overwhelmed or depleted, thereby having significant implications for the interpretation of toxicological data in rodents (Thompson et al., 2013). For example, Table 2 (adapted from Proctor et al. (2012)) illustrates a manner in which species-differences in Cr-VI reduction capacity may be interpreted. If one examines the reducing capacity of only one of the kinetic reactions, it may be concluded that mice are more susceptible than rats, since when compared per drinking event, rats have about 50% higher reducing capacity. For example, by the original model at 21 mg/L a mouse is predicted to consume 130% of its reducing capacity per drinking event while the rat is predicted to consume 94% of its capacity. Likewise for our revised model the reducing capacity of the "fast" pool in the rat, relative to a drinking event, is predicted to be about twice that of the "fast" pool in the mouse. However if both the "fast" and "slow" reducing capacities estimated using the revised model are added together (neglecting the impact of the third "very slow" reaction with undetermined capacity), the difference in susceptibility becomes negligible. The revised model suggests that under the complex physiological conditions of the stomach, a combination of slow, fast, and very slow reduction reactions will be simultaneously competing with each other and the gastric emptying process. However the reducing capacities are just one of many factors impacting the reduction and systemic uptake of Cr-VI.

Table 1
Final kinetic parameters for Cr-VI reduction in gastric juice of rats and mice (3-pools) and humans (1-pool).

Symbol	Definition (units)	Value		
Species-independent parameters				
K_{11}	Equilibrium constant (M^{-1})	1080		
K_{22}	Equilibrium constant (M^{-1})	132		
K_{21}	Equilibrium constant (M^{-1})	13.2		
K_{32}	Equilibrium constant (M^{-1})	15.2		
f	Fractional reactivity of CrO_4^{2-} (*no units*)	0.0025		
		Rat	Mouse	Human
Species-specific parameters				
k_f or k_1	Fast binary rate constant (L/mg-min)	2.4[a]	2.4	0.62
k_s	Slow binary rate constant (L/mg-min)	0.15[a]	0.15	–
k_{vs}	Very slow first-order constant (1/min)	0.058	0.044	–
$R_{0,f}$ or $R_{0,1}$	Fast reducing agent pool size (mg/L)	4.1	2.9	10
$R_{0,s}$	Slow reducing agent pool size (mg/L)	18	31	–

[a] k_f and k_s for the rat where fixed at the values estimated for the mouse.

Discussion

The work presented here is an extension of the model by Proctor et al. (2012) and Kirman et al. (2013), and incorporates mechanistic reaction schemes to describe ex-vivo Cr-VI reduction kinetics in humans and rodents. The model was chosen to balance parsimony with mechanistic complexity. The revised Cr-VI reduction model is more complex than the previous models in two ways: the assumption of multiple reducing agent pools and a more elaborate description of pH-dependence. Predicting dosimetry under long-term exposure conditions is desirable, so the reduction model should accurately predict the experimental data beyond the first 20 min, at least to the 60 min time-point for which data are available, across the tested concentration range. For comparison, the NTP bioassay exposed mice and rats to 5–180 mg/L Cr-VI equivalents (NTP, 2008). Ingested water will be diluted into the entire gastric contents, so the relevant concentration will be less than in the drinking water, making the lower end of the concentration range evaluated here most important. The analysis of which dose

Table 2
Comparison of mouse and rat Cr6 stomach loading and reducing capacity (adapted from Proctor et al. (2012)).

Cr6 DW (mg/L)	Water intake per event (L)	Cr6 intake per event (mg)	Reducing capacity (mg/mL)	Stomach contents (mL)	Total reducing equiv. (mg)	Cr6 intake per event as % of reducing capacity		
						Orig.	Fast	Fast + slow
Mouse								
0.1	0.0002	0.00002	0.0166 (original)[a]	0.2	0.0033 (original) 0.00058 (fast)	0.6	3.4	0.3
1.4		0.00028	0.0029 (fast)[b]		0.00678 (fast + slow)	8.5	48.3	4.1
5		0.001	0.0339 (fast + slow)[c]			30	172	15
21		0.0042				130	724	62
60		0.012				360	2069	177
180		0.036				1100	6207	531
Rat								
0.1	0.0007	0.00007	0.0157 (original)[a]	1	0.0157 (original) 0.0041	0.4	1.7	0.3
1.4		0.00098	0.0041		(fast)	6.2	24	4.4
5		0.0035	(fast)[b]		0.0221	22	85	16
21		0.0147	0.0221 (fast + slow)[c]		(fast + slow)	94	360	67
60		0.042				270	1024	190
180		0.1274				810	3107	577

[a] Original published value.
[b] R_{0f} from Table 1.
[c] The sum of R_{0f} and R_{0s} from Table 1.

levels might overcome the total reducing capacity depends on a good estimate of that capacity, which is provided by the higher concentration ex vivo data. For humans the relevant range is much lower. The highest level reported in drinking water was 0.097 mg/L (as of March 3, 2014), with most samples falling below 0.003 mg/L (3 ppb) (USEPA, 2014). While the concentration range examined by Kirman et al. (2013) and re-evaluated here is orders of magnitude higher, the changes proposed for the human reduction model were not in the number of reducing agent pools (which would only be important at higher concentrations), but in the pH-dependence.

In both Figs. 2 and 3 the improvement in model fit to the total data set is clear. A slightly simpler variation considered used only 2 pools of reducing agent, but as shown in the 14 ppm data set in Fig. 2, the addition of a third pool (using a single first-order rate constant) provides a significant additional improvement at the higher concentration. Similar improvements occur at 15 and 40 ppm in the mouse gastric reduction (data in Fig. 3, but 2-pool model not shown). On the other hand introducing two more parameters, specifically a binary constant and reduction capacity for the third pool, provided a negligible improvement over the results shown, with large uncertainty in the third pool capacity. That multiple pools of reducing agents (electron donors) exist in gastric juice, including ascorbate, NADH, and glutathione, was noted by Proctor et al. (2012). Thus the revised model is also consistent with the biochemical constituents in gastric juice.

A mathematical model can be overly complicated if it contains parameters that are not identifiable given the existing data, especially if this lack of identifiability leads to uncertainty in model predictions. Therefore a certain level of parsimony is desirable. But parsimony alone would lead one to choose a classical pharmacokinetic (PK) model over a physiologically-based pharmacokinetic (PBPK) model, since the former is clearly simpler and has fewer parameters. The counterbalancing principle that has led to the use of PBPK models in risk assessment is mechanistic plausibility, which is expected to increase a model's reliability when used to predict data outside of the observed range and conditions. PBPK models do not introduce many more parameters in the absence of additional data. They make use of data on tissue volumes, blood flows, and respiration rate, in addition to chemical-specific data. While the PBPK model structure is more elaborate than a classical PK model, together with the physiological parameters that are generally not fitted during model calibration, the resulting PBPK model predictions are much less sensitive to the fitted chemical-specific parameters than a classical PK model. Hence the uncertainty due to its fitting to a limited data set is constrained. For example, hepatic metabolism in a PBPK model is limited by blood-flow and, ultimately, inhalation rate for inhaled gases. Therefore, the impact of uncertainty in the Vmax for hepatic metabolism is minimal for large values of Vmax.

Likewise when there are data that a model does not fit and these discrepancies are indicative of systematic errors in a model – i.e., trends with experimental conditions such as time or concentration not captured by a model – and elaborations of the model improve its ability to capture these trends, then such elaborations can improve a model's predictive reliability. If a more complex model structure is obtained from mechanistic knowledge of specific processes involved, and if that knowledge derives from other experimental data, then added model complexity can improve predictability (rather than increasing uncertainty). This is particularly true if underlying parameter values are derived from independent, supporting experimental data. For the revised reduction model, three of the four equilibrium constants that determine the speciation (for reactions 1–4) were identified independently from other experimental data and not adjusted here. The revised model now accurately captures the variation in reduction rate with pH as shown in Figs. 4 and 5. The rate and extent of Cr-VI reduction predicted for humans vs. rodents will directly impact the estimated cancer risk in humans. Therefore we sought to improve the ability of the gastric-juice reduction models to fit the reduction data of Proctor et al. (2012) and Kirman et al. (2013) in order to more accurately estimate the relative dosimetry and hence risk in humans. The impact of these changes can only be evaluated in the context of a PBPK model which integrates gastric reduction in various GI compartments with rates of ingestion, cofactor replenishment, Cr absorption, etc. Those results will be described in a subsequent publication. However, independent of the extent to which use of the revised reduction model might quantitatively change the exposure–internal-dose relationship, that the revised model better describes the overall data set with minimal additional parameters should improve the level of confidence in those predictions.

The ex vivo reduction model described here can be incorporated into 1) a gastrointestinal tract model and, subsequently 2) a whole-body PBPK model (Fig. 1). While preliminary results regarding species differences were obtained using only the ex vivo reduction kinetics (Table 1), a more complete analysis can only be done by taking into account gastric dynamics and differences in systemic absorption. Gastric and whole-body PBPK models defining the processes specific to Cr(VI) were previously described by (Kirman et al., 2013; Kirman et al., 2012). Updating these models to incorporate the revised reduction kinetics is the subject of ongoing work.

Disclaimer

The views expressed in this paper are those of the authors and do not necessarily represent the views or policies of the U.S. Environmental Protection Agency.

Acknowledgments

The authors thank Drs. Sean M. Hays (Summit Toxicology), Christopher R. Kirman (Summit Toxicology), and Deborah M. Proctor (ToxStrategies, Inc.), along with their colleagues, for providing the original chromium reduction data and model spreadsheets on which this analysis is based, as well as helpful discussions during the development of these results. They also thank Drs. Paul White, Catherine Gibbons, Ravi Subramaniam, Ted Berner, Susan Rieth, Elaina Kenyon, and Cecilia Tan (U.S. EPA) for helpful comments and discussions. The authors gratefully acknowledge the presenters and other participants in U.S. EPA's Hexavalent Chromium Workshop, Sept. 19 and 25, 2013 (http://www.epa.gov/iris/irisworkshops/cr6/index.htm).

Appendix A. Supplementary data

Supplementary data to this article can be found online at http://dx.doi.org/10.1016/j.taap.2014.08.010.

References

Brito, F., Ascanio, J., Mateo, S., Hernández, C., Araujo, L., Gili, P., Martín-Zarza, P., Domínguez, S., Mederos, A., 1997. Equilibria of chromate(VI) species in acid medium and ab initio studies of these species. Polyhedron 16 (21), 3835–3846. http://dx.doi.org/10.1016/s0277-5387(97)00128-9.

De Flora, S., D'Agostini, F., Balansky, R., Micale, R., Baluce, B., Izzotti, A., 2008. Lack of genotoxic effects in hematopoietic and gastrointestinal cells of mice receiving chromium(VI) with the drinking water. Mutat. Res. 659 (1–2), 60–67. http://dx.doi.org/10.1016/j.mrrev.2007.11.005.

DeSesso, J.M., Jacobson, C.F., 2001. Anatomical and physiological parameters affecting gastrointestinal absorption in humans and rats. J. Publ. Br. Ind. Biol. Res. Assoc. 39 (3), 209–228.

Febel, H., Szegedi, B., Huszar, S., 2001. Absorption of inorganic, trivalent and hexavalent chromium following oral and intrajejunal doses in rats. Acta Vet. Hung. 49 (2), 203–209.

Kararli, T.T., 1995. Comparison of the gastrointestinal anatomy, physiology, and biochemistry of humans and commonly used laboratory animals. Biopharm. Drug Dispos. 16 (5), 351–380.

Kerger, B.D., Paustenbach, D.J., Corbett, G.E., Finley, B.L., 1996. Absorption and elimination of trivalent and hexavalent chromium in humans following ingestion of a bolus dose in drinking water. Toxicol. Appl. Pharmacol. 141 (1), 145–158. http://dx.doi.org/10.1006/taap.1996.0271.

Kirman, C.R., Hays, S.M., Aylward, L.L., Suh, M., Harris, M.A., Thompson, C.M., Haws, L.C., Proctor, D.M., 2012. Physiologically based pharmacokinetic model for rats and mice orally exposed to chromium. Chem. Biol. Interact. 200 (1), 45–64. http://dx.doi.org/10.1016/j.cbi.2012.08.016.

Kirman, C.R., Aylward, L.L., Suh, M., Harris, M.A., Thompson, C.M., Haws, L.C., Proctor, D.M., Lin, S.S., Parker, W., Hays, S.M., 2013. Physiologically based pharmacokinetic model for humans orally exposed to chromium. Chem. Biol. Interact. 204 (1), 13–27. http://dx.doi.org/10.1016/j.cbi.2013.04.003.

NTP (2008). Toxicology and carcinogenesis studies of sodium dichromate dihydrate (Cas No. 7789-12-0) in F344/N rats and B6C3F1 mice (drinking water studies). NTP TR 546, NIH Publication No. 08–5887, pp. 1–192. National Toxiciology Program, Research Triangle Park, NC

Proctor, D.M., Suh, M., Aylward, L.L., Kirman, C.R., Harris, M.A., Thompson, C.M., Gurleyuk, H., Gerads, R., Haws, L.C., Hays, S.M., 2012. Hexavalent chromium reduction kinetics in rodent stomach contents. Chemosphere 89 (5), 487–493. http://dx.doi.org/10.1016/j.chemosphere.2012.04.065.

Stout, M.D., Herbert, R.A., Kissling, G.E., Collins, B.J., Travlos, G.S., Witt, K.L., Melnick, R.L., Abdo, K.M., Malarkey, D.E., Hooth, M.J., 2009. Hexavalent chromium is carcinogenic to F344/N rats and B6C3F1 mice after chronic oral exposure. Environ. Health Perspect. 117 (5), 716–722. http://dx.doi.org/10.1289/ehp.0800208.

Thompson, C.M., Proctor, D.M., Suh, M., Haws, L.C., Kirman, C.R., Harris, M.A., 2013. Assessment of the mode of action underlying development of rodent small intestinal tumors following oral exposure to hexavalent chromium and relevance to humans. Crit. Rev. Toxicol. 43 (3), 244–274. http://dx.doi.org/10.3109/10408444.2013.768596.

USEPA, 2014. The third Unregulated Contaminant Monitoring Rule (UCMR 3) occurrence data. U.S. Environmental Protection Agency, Washington, DC, (Available at: http://water.epa.gov/lawsregs/rulesregs/sdwa/ucmr/data.cfm#ucmr2013).